HHS Public Access

Author manuscript

Neuroimage. Author manuscript; available in PMC 2016 August 15.

Published in final edited form as:

Neuroimage. 2015 August 15; 117: 222–229. doi:10.1016/j.neuroimage.2015.05.054.

Decoupling of structural and functional brain connectivity in older adults with white matter hyperintensities

Y.D. Reijmer[a], **A.P. Schultz**[b,d], **A. Leemans**[e], **M.J. O'Sullivan**[f], **M.E. Gurol**[a], **R. Sperling**[a,b,d,g], **S.M. Greenberg**[a], **A. Viswanathan**[a], and **T. Hedden**[c,d]

[a]Dept. of Neurology, Massachusetts General Hospital, Harvard Medical School, Boston, MA, USA [b]Dept. of Psychiatry, Massachusetts General Hospital, Harvard Medical School, Boston, MA, USA [c]Dept. of Radiology, Massachusetts General Hospital, Harvard Medical School, Boston, MA, USA [d]Athinoula A. Martinos Center for Biomedical Imaging, Massachusetts General Hospital, Charlestown, MA, USA [e]Image Sciences Institute, University Medical Center Utrecht, Utrecht, the Netherlands [f]Dept. of Basic and Clinical Neuroscience, Institute of Psychiatry, Psychology & Neuroscience, King's College London, UK [g]Dept. of Neurology, Brigham and Women's Hospital, Harvard Medical School, Boston, MA, USA

Abstract

Age-related impairments in the default network (DN) have been related to disruptions in connecting white matter tracts. We hypothesized that the local correlation between DN structural and functional connectivity is negatively affected in the presence of global white matter injury. In 125 clinically normal older adults, we tested whether the relationship between structural connectivity (via diffusion imaging tractography) and functional connectivity (via resting-state functional MRI) of the posterior cingulate cortex (PCC) and medial prefrontal frontal cortex (MPFC) of the DN was altered in the presence of white matter hyperintensities (WMH). A significant correlation was observed between microstructural properties of the cingulum bundle and MPFC-PCC functional connectivity in individuals with low WMH load, but not with high WMH load. No correlation was observed between PCC-MPFC functional connectivity and microstructure of the inferior longitudinal fasciculus, a tract not passing through the PCC or MPFC. Decoupling of connectivity, measured as the absolute difference between structural and functional connectivity, in the high WMH group was related to poorer executive functioning and memory performance. These results suggest that such decoupling may reflect reorganization of functional networks in response to global white matter pathology and may provide an early marker of clinically relevant network alterations.

Corresponding author Yael D Reijmer, PhD J.P. Kistler Stroke Research Center 175 Cambridge Street, Suite 300, Boston, Massachusetts, USA, 02114 yreijmer@mgh.harvard.edu, Tel: (617) 643-7597.

Conflicts of interest

There are no actual or potential conflicts of interest to disclose.

Keywords

functional MRI; diffusion tensor imaging; connectivity; cognition; aging; white matter hyperintensities

1. Introduction

Aging is associated with reduced coherence in large-scale functional networks (Andrews-Hanna et al., 2007), such as the default network (DN) (Damoiseaux et al., 2008; Ferreira and Busatto 2013; Lustig et al., 2003). Functional connectivity within the DN measured by resting-state functional MRI (fMRI) has been associated with cognitive performance (Andrews-Hanna et al., 2007; Raichle et al., 2001; Ward et al., 2014) and impaired DN connectivity has been linked to mild cognitive impairment and Alzheimer's disease (Chhatwal and Sperling 2012; Greicius et al., 2004).

Age-related impairments in functional networks are often hypothesized to arise from disruptions in connecting white matter tracts (Damoiseaux and Greicius 2009; Johansen-Berg 2009). Support for this hypothesis comes from diffusion tensor imaging (DTI) studies showing compromise of white matter integrity with increasing age (Charlton et al., 2006; Pfefferbaum et al., 2005; Salat et al., 2005). Fiber tracts affected in aging include long-range association bundles running between major nodes of the DN, such as the cingulum bundle (Greicius et al., 2009). The superior part of the cingulum bundle primarily consists of short arcuate fibers along which information is relayed between the frontal cortex and posterior regions including the precuneus and posterior cingulate (Jones et al., 2013, for review). Functional connectivity between the anterior and posterior nodes of the DN has been shown to positively correlate with cingulum integrity, suggesting a local relationship between structural and functional connectivity measures in healthy adults (Andrews-Hanna et al., 2007; Honey et al., 2009; van den Heuvel et al., 2008).

Since major nodes of the DN are highly connected with other parts of the brain, it can be inferred that local structure-function relationships also depend on the quality of the surrounding network connections. For example, functional connectivity between two nodes of the DN may be reduced by disruption of functional inputs from network neighbors, despite relative intactness of the major connecting fiber bundle (Honey et al., 2009). Our overarching hypothesis was that white matter brain injury in remote regions of a network can impact the coupling of direct structural and functional connectivity measures, resulting in a *decoupling* of structural and functional connectivity (Wang et al., 2014). That is, for a given set of connected nodes, the correlation between structural and functional connectivity is expected to be weaker in individuals with white matter injury in the surrounding fiber tracts compared to those without such injury. Decoupling of structural and functional connectivity has been observed in patients with large-scale brain disruptions such as schizophrenia (Skudlarski et al., 2010) and epilepsy (Zhang et al., 2011) and has been related to clinical symptoms (Skudlarski et al., 2010).

We tested our hypothesis in clinically normal older adults with high white matter hypertensities (WMH) on MRI, a common marker of white matter injury (Hedden et al.,

2014; Leritz et al., 2014; O'Sullivan et al., 2001; Vernooij et al., 2009). Given the potential complexity of the relationship, we focused our analysis on two well-described nodes of the DN network: the posterior cingulate cortex (PCC) and medial prefrontal cortex (MPFC), between which information is passed along the cingulum bundle. Specifically, we hypothesized that the correlation between cingulum structure (assessed with DTI) and PCC-MPFC functional connectivity (assessed with resting-state fMRI) would be weaker in individuals with relatively high WMH load compared to those with low WMH load. To examine the topographic specificity of this association, we included a control fiber tract not passing through either the PCC or MPFC (the inferior longitudinal fasciculus). We hypothesized that the structural properties of this control tract would not be correlated with PCC-MPFC functional connectivity independent of WMH load. Finally, we hypothesized that the extent of structural and functional decoupling in the high WMH group would be related to worse cognitive performance.

2. Materials and methods

2.1 Sample characteristics

Participants were 125 (63% females; aged 65-87 years) community-dwelling clinically normal older adults participating in the Harvard Aging Brain Study, an ongoing longitudinal study in the baseline assessment phase at the time of this analysis. Participants were excluded if they received a Clinical Dementia Rating (CDR) greater than 0, scored less than 27 on the Mini-Mental State Examination (Folstein et al., 1975), had been previously diagnosed with a neurological or psychiatric condition, had a history of head trauma, or presented with any safety or comfort (e.g. claustrophobia) contraindications for magnetic resonance imaging (MRI). For the current study we included all subjects with a complete set of data that passed quality assessment (see below) for diffusion tensor imaging, resting-state functional MRI (fMRI), and cognitive data as of August 2013. Ninety-six of the participants presented with hypertension, defined as systolic blood pressure ≥140, diastolic blood pressure ≥90, or the use of antihypertensive medication; 3 participants were unclassified on hypertension due to missing data on one or more symptom measurements. All participants provided informed consent in accordance with protocols approved by the Partners Healthcare Inc. Institutional Review Board. Subjects in this analysis were included in previous reports of relationships between WMH or DTI and cognition and resting-state fMRI data and cognition (Hedden et al., 2012; Hedden et al., 2014; Ward et al., 2014). The tract-based DTI metrics and the relationships between DTI and resting-state fMRI have not been previously reported.

2.2 Cognitive assessment

Participants completed an extensive neuropsychological battery including tasks assessing executive functioning, processing speed, and episodic memory. In brief, measures associated with executive functioning included letter fluency (F, A, S), category fluency (animals, vegetables, fruits), the Letter-Number Sequencing subtest of the Wechsler Adult Intelligence Scale-III, the Digit Span Backward subtest of the WAIS revised (WAIS-R), the Self-Ordered Pointing task, the across-block switching reaction time from the Number-Letter task, a modified Flanker task, and the Trail Making Test Form B minus Form A. Measures

associated with episodic memory included cued recall from the Face-Name Associative Memory Exam, delayed recall from the Six-Trial Selective Reminding Test, and List 2 free recall from the Memory Capacity Test. Measures associated with processing speed included the nonswitching blocks from the Number-Letter task, the Trail Making Test Form A, and the digit-symbol subtest of the WAIS-R. Detailed description of the cognitive measures and calculation of the composite scores using confirmatory factor analysis are reported in Hedden et al. (2012). Composite scores of each cognitive domain were transformed into z-scores based on the mean and standard deviation of the present study sample prior to analysis.

2.3 MRI data acquisition

All MRI data were collected on a Siemens Trio-TIM 3 Tesla scanner equipped with a 12-channel phased-array head coil. Head motion was restrained with a foam pillow and extendable padded head clamps. The scan protocol included two back-to-back resting-state fMRI scans (6 min. per run). Data were acquired using a gradient-echo echo-planar imaging sequence sensitive to BOLD contrast with the following parameters: repetition time (TR) = 3000ms, echo time (TE) = 30ms, flip angle = 85°, field-of-view (FOV) = 216×216mm, matrix = 72×72, and 3 mm^3 voxels. 124 volumes were acquired in each run. Participants were instructed to lie still, remain awake, and keep eyes open. High-resolution 3D T1-weighted multi-echo magnetization-prepared, rapid acquisition gradient echo anatomical images were collected with the following parameters: TR=2200 ms; multi-echo TEs=1.54 ms, 3.36 ms, 5.18 ms, and 7 ms; FA = 7°, 4× acceleration, 1.2 mm^3 voxels. Fluid attenuation inversion recovery (FLAIR) images for visualization of white matter lesions were collected with the following parameters: TR= 6000 ms, TE = 454 ms, TI = 2100 ms, 1 × 1 × 1.5mmvoxels. Diffusion weighted images were acquired using a single shot spin echo planar imaging sequence, with a TR=6230, TE=84 ms, a flip angle of 90°, FOV: 256×256×128 mm^3; acquired isotropic voxel size 2 mm^3, 30 isotropically distributed diffusion-sensitizing gradients with a b-value of 700 s/mm^2 and 5 non-diffusion weighted images (b = 0 s/mm^2) (Jones and Leemans 2011).

2.4 Quantification of WMH and brain atrophy

WMH load was visually rated on FLAIR images according to the Fazekas rating scale (range 0-3) (Fazekas et al., 1987). The Fazekas WMH scale was used to define the low and high WMH groups and to facilitate interpretation because it indicates the clinical severity of WMH load. A Fazekas score of 0 or 1 (i.e. none, periventricular caps, pencil thin lining, and/or punctate deep WMH lesions <10 mm) was considered ‘low WMH load’ and a score of 2 or 3 (i.e. smooth halo, beginning or large confluent lesions ≥10 mm) was considered as ‘high WMH load’ as previously reported (Gouw et al., 2006; Homayoon et al., 2013). The Fazekas scores corresponded well (Spearman's ρ=0.81) with previously reported results obtained using an automated WMH segmentation method (Hedden et al., 2012). We note that no subjects received a Fazekas score of 0, as all subjects exhibit some degree of normal age-related periventricular or punctate WMH lesions.

Total brain volumes were obtained from T1-weighted GRE images using the previously validated Freesurfer software (http://surfer.nmr.mgh.harvard.edu) (Fischl and Dale 2000).

All segmented volumes were visually inspected for segmentation errors. To account for between subject differences in head size, brain volumes were expressed as a percentage of intracranial volume.

2.5 DTI Data Processing

The diffusion MRI data sets were processed and analyzed in *ExploreDTI* (http://www.exploredti.com)(Leemans et al., 2009). Data preprocessing, including correction of subject motion and eddy current–induced geometric distortions and tensor estimation, was performed as described previously (Leemans and Jones 2009; Reijmer et al., 2012).

All brain scans were rigidly normalized to Montreal Neurological Institute (MNI) space during the motion-distortion correction step to maximize the uniformity of brain angulation across subjects (Rohde et al., 2004). Whole-brain deterministic streamline fiber tractography was performed using constrained spherical deconvolution-based fiber tractography (Jeurissen et al., 2011; Tax et al., 2014; Tournier et al., 2007). Fibers were reconstructed by starting seed samples uniformly distributed throughout the data at 2 mm isotropic resolution with a maximum deflection angle of 45° and a fiber orientation distribution threshold 0.1, and maximum harmonic degree of 4 (Tournier et al., 2007).

The superior segment of the cingulum bundle and right inferior longitudinal fasciculus (ILF) were delineated from the whole-brain tractography maps. The ILF was selected as a control tract because it is an association tract not passing through the PCC or MPFC. In addition, the majority of ILF fibers have relatively low curvature, thereby not complicating reconstruction. Regions of interest (ROI) for ‘tract selection’ and ‘tract exclusion’ were placed manually on the color-coded FA map of one subjects' brain in MNI space according to a priori information on tract location (Catani and Thiebaut de Schotten 2008). ROIs were automatically transformed to every other data set using non-rigid B-spline registration (Lebel et al., 2008). All tract reconstructions were visually inspected and spurious tracts were excluded manually by an experienced rater (YDR) blinded to WMH status. High intra- and interrater reliability of segmenting fiber bundles using this approach has been demonstrated in previous studies (Kristo et al., 2013). The mean fractional anisotropy (FA) and mean diffusivity (MD) were calculated for each white matter tract. In addition, we calculated the mean FA and mean MD of the whole white matter excluding the cingulum bundle. To this end, for each individual, we removed the streamlines of the superior segment of the cingulum bundle from the whole-brain fiber tractography results and calculated the mean FA and MD of the remaining streamlines.

2.6 fMRI Data Processing

All resting state data were processed using SPM8 (http://www.fil.ion.ucl.ac.uk/spm/; version r4290). The first four volumes of each run were discarded to allow for T1 equilibration effects. Each run was slice- time corrected, realigned to the first volume of the run with INRIAlign (Freire and Mangin 2001), normalized to the MNI 152 EPI template and smoothed with a 6 mm FWHM Gaussian kernel. Following these standard preprocessing steps, additional processing known to be beneficial for functional connectivity MRI analysis was conducted. These included (sequentially, and in this order) (1) regression of realignment

parameters (plus first derivatives) to reduce movement artifacts on connectivity (2) temporal band-pass filtering (second order Butterworth filter) to focus the analysis on frequencies in the 0.01-0.08 Hz band and (3) we regressed out the average signal from white matter, ventricles, and global signal (plus first derivatives) after application of the band-pass filter (Fox et al., 2006; Van Dijk et al., 2010). All subjects included in the present analysis met criteria of global signal to noise (SNR) greater than 115, average movement less than .15 mm/TR, and number of outlier volumes less than 20. Outlier volumes were identified as volumes where global signal was greater than or less than 2.5 standard deviations of the entire run, where movement was greater than .75 mm between TRs, or where rotation was more than 1.5 degrees between TRs. Outlier volumes were removed from the analyses after preprocessing but prior to computing connectivity maps.

2.7 Functional connectivity analysis

A DN template, created from an independent set of 675 young subjects using a factor rotation method (Schultz et al., 2014), was used to define DN regions of interest. The DN template map was thresholded to identify individual functional clusters corresponding to 6 functional nodes (threshold=0.6*peak of each cluster). Figure 1 shows a label map of the regions. All regions represent areas of DN connectivity of at least $p < 0.001$ false-discovery rate (FDR) corrected. For each subject, functional connectivity between the average time-course from the PCC ROI and MPFC ROI was calculated as the Pearson's correlation between the two time-series. A Fisher's r-to-z transformation was used to improve the normality of the partial correlation coefficients.

2.8 Decoupling measure

PCC-MPFC decoupling was defined as the absolute difference between the z-scores of PCC-MPFC functional connectivity and cingulum MD. We selected MD because it has shown the most robust relationships with clinical outcome in adults with WMH (O'Sullivan et al., 2001; Vernooij et al., 2009) and it showed the strongest association with functional connectivity in the below mentioned analysis. Z-scores for cingulum MD were reverse scaled (multiplied by −1) such that higher scores indicate better connectivity. Z-scores for functional connectivity were adjusted for mean movement per session, SNR, and the number of outlier volumes removed from each fMRI data set. The absolute difference between the structural and functional z-scores was taken. Hence, a score near 0 on the decoupling measure (low decoupling) indicates that an individual has a similar position within the sample on both structural and functional connectivity measures. A large positive score (high decoupling) indicates that the individual has relatively high structural connectivity but relatively low functional connectivity, or relatively low structural connectivity but relatively high functional connectivity. Hence, the score does not distinguish between these two forms of decoupling. The decoupling measure was log transformed to obtain a normal distribution.

2.9 Statistical Analysis

Patient characteristics including MRI measures of structural and functional connectivity and cognitive performance were compared between individuals with low versus high WMH load using independent samples T-tests for continuous variables and Chi-square tests for proportions.

To examine whether cingulum MD or FA was related to PCC-MPFC functional connectivity and whether this relationship was modulated by WMH load we performed separate analyses of variance (ANOVA) with PCC-MPFC functional connectivity as the dependent variable. Effects of interest in the model were main effects for WMH group (low/high), cingulum MD or FA, and the interaction of Cingulum MD or FA*WMH group. To ensure that the connectivity metric was not impacted by data quality (Power et al., 2012; Van Dijk et al., 2012), we entered the following data quality variables as covariates: mean movement per session, SNR, and the number of outlier volumes removed from each fMRI data set. To test whether the relationship between PCC-MPFC functional connectivity and white matter integrity was specific to these connections and not attributable to more global variations in functional connectivity of the DN or in white matter structure, we entered as covariates the mean connectivity among the DN nodes excluding the PCC and MPFC, MD or FA of the ILF, and mean MD or FA of all white matter *excluding* the cingulum bundle. We also examined the interaction of ILF MD or FA*WMH group, with the hypothesis that integrity in this tract (which does not connect directly to either the PCC or MFPC) would not be differentially related to PCC-MPFC connectivity across the WMH groups. As additional covariates, we entered age, sex, total brain volume, and hypertension. We also examined a simplified model entering only covariates for age, sex, and the data quality variables to determine whether any observed relationships between PCC-MPFC functional connectivity and cingulum integrity were potentially induced by the other covariates.

For each significant interaction effect with WMH group we subsequently examined the strength of the association with functional PCC-MPFC connectivity within each group separately using the simplified model in a linear regression analysis.

Lastly, we examined whether decoupling of structural and functional connectivity was associated with worse cognitive functioning. Decoupling of PCC-MPFC functional connectivity and cingulum MD was quantified by a single measure (see Methods) and used as an independent variable to predict processing speed, executive functioning, and episodic memory in linear regression analyses controlling for age and sex.

3. Results

Table 1 shows the group characteristics of the study sample. Individuals with high WMH load (n=61) were older, had lower PCC-MPFC functional connectivity, lower tract FA, and higher tract MD than elderly with low WMH load (n=64). The age-adjusted between-group difference in MD was larger for the total white matter surrounding the cingulum bundle than for the cingulum bundle itself (Table 2), which in line with the periventricular distribution of WMH. See Inline Supplementary Figure 1 for the distribution of WMH within the study sample. Total tract volumes of the cingulum bundle and ILF were not significantly different between groups ($p>0.33$). Between-group differences in processing speed and executive functioning remained significant after controlling for age, sex, and years of education ($p<0.05$).

3.1 Structural-functional coupling in individuals with low and high WMH load

We examined cingulum MD and FA in separate ANOVAs. In the whole study sample, there was a significant main effect of cingulum MD on PCC-PMFC functional connectivity ($F_{1,107}$=4.28, p=0.041), after controlling for all covariates (see Methods). Supporting our hypothesis, the association between cingulum MD and PCC-MPFC functional connectivity differed across the low and high WMH groups (cingulum MD*WMH group interaction effect: $F_{1,107}$=4.59, p=0.035). Notably, neither the main effect of ILF MD ($F_{1,107}$=0.51, p=0.476), nor the interaction of ILF MD*WMH group were significant ($F_{1,107}$=0.26, p=0.613). The only covariate with a significant effect was mean functional connectivity among the DN nodes excluding the PCC and MPFC ($F_{1,107}$=14.96, p<0.001). In the simplified model, there was again a significant main effect for cingulum MD ($F_{1,116}$=10.23, p=0.002) and for WMH group ($F_{1,116}$=5.05, p=0.027), as well as a significant cingulum MD*WMH group interaction ($F_{1,116}$=4.65, p=0.033).

Follow-up regression analyses using the simplified model and stratified for WMH group showed that increased cingulum MD, indicating decreased structural connectivity, was associated with decreased PCC-MPFC functional connectivity in the low WMH group (standardized β= −0.44, p<0.001), but this relationship was absent in the high WMH group (β= 0.03, p=0.806; Figure 3).

In the FA model after controlling for all covariates (see Methods), there were no significant main effects of cingulum FA on PCC-MPFC functional connectivity ($F_{1,107}$=2.59, p=0.111) or WMH group ($F_{1,107}$=0.19, p=0.665), and no significant cingulum FA*WMH group interaction ($F_{1,107}$=0.81, p=0.370). Additionally, no effects involving ILF FA or the mean FA of all white matter excluding the cingulum bundle were significant (smallest p=0.24). The only covariates with a significant effect were mean connectivity among the DN nodes excluding the PCC and MPFC ($F_{1,107}$=13.84, p<0.001) and total brain volume ($F_{1,107}$=4.94, p=0.028). In the simplified model, there was a significant main effect for cingulum FA on PCC-MPFC functional connectivity ($F_{1,116}$=5.95, p=0.016), but no significant effect for WMH group ($F_{1,116}$=0.98, p=0.325), or for the cingulum FA*WMH group interaction ($F_{1,116}$=1.31, p=0.254).

3.2 Structural-functional decoupling and cognition

When expressing the decoupling between PCC-MPFC functional connectivity and cingulum MD as a single score (see Methods), we found no association between the extent of decoupling and cognitive functioning in the low WMH group (all cognitive domains: β > −0.124; p>0.327). As follows from the results above, decoupling of PCC-MPFC connectivity within the low WMH group was close to zero and lower than in the high WMH group (low WMH: 0.75 ± 0.56, high WMH: 1.11 ± 0.84, p=0.038). In the high WMH group however, greater decoupling of PCC-MPFC connectivity was related to worse performance for executive functioning (β(95% CI)= −0.36 (−0.61 to −0.11), p=0.006), and episodic memory (β=−0.36 (−0.60 to −0.12), p=0.004), but not for processing speed (β=−0.17 (−0.44 to 0.10), p=0.206) (Figure 4). By contrast, individual measures of structural and functional connectivity were not significantly related to executive functioning or episodic memory in the high WMH group (p>0.08; see Inline Supplementary Table 1). The present analyses

combine both forms of decoupling in which structural connectivity is greater than functional connectivity and vice versa. Indeed, both directions of decoupling were related to worse cognitive functioning as shown in Supplementary Figure 2.

4. Discussion

Our primary finding demonstrates a correlation between microstructural properties of the cingulum bundle and MPFC-PCC functional connectivity in individuals with low WMH load, but a decoupling of this relationship in individuals with high WMH load. The extent of decoupling in the high WMH group was related to worse executive functioning and episodic memory performance.

Our results extend previously described structure-function relationships in young adults (Honey et al., 2009; van den Heuvel et al., 2008) and in older adults (Andrews-Hanna et al., 2007) by showing that the coupling of structural and functional connectivity between network nodes is reduced in the presence of global white matter pathology. Furthermore, our results indicate that this link between structural and functional connectivity is topographically specific. To demonstrate this, we examined the tissue microstructure in a control tract not passing through the PCC or MPFC (the ILF) and in the whole white matter excluding the cingulum bundle. We additionally controlled for functional connectivity in other parts of the network. In line with our hypotheses, no significant association was observed between PCC-MPFC functional connectivity and these control measures, suggesting that the observed correlation between PCC-MPFC functional connectivity and cingulum microstructure is not simply driven by more general variations in global white matter health or BOLD fluctuations.

The observation of a diminished correlation between PCC-MPFC functional connectivity and cingulum structure in older adults with high WMH load likely results from interweaving mechanisms underlying network dynamics. The PCC and MPFC participate in large-scale brain networks. Functional connectivity between the PCC and MPFC depends therefore on the structural tissue characteristics of direct connections as well as of indirect connections linking to neighboring nodes (Honey et al., 2009). This may imply that aberrant neuronal input from brain regions elsewhere in the network can reduce functional connectivity between two target regions, despite relative intactness of the major white matter tract between those regions. Our data indicates potential support for this possibility in that some individuals with high WMH load had relatively preserved cingulum microstructure but nonetheless exhibited lower than average functional connectivity (Figure 3, lower left). In addition, we observed that some individuals with high WMH load exhibited average levels of functional connectivity despite impaired cingulum integrity (Figure 3, upper right). This preserved functional connectivity despite abnormal cingulum structure, may be explained by the utilization of alternate, less affected, white matter pathways. It is also possible that white matter disease has a differential impact on measures of structural and functional connectivity. Vascular, neuronal, and axonal abnormalities that underlie macroscopic WMH likely have differential consequences for the BOLD response underlying functional connectivity and diffusion parameters used to measure microstructural tissue properties (Wang et al., 2014). Understanding the complex dynamics between global white matter

pathology and brain connectivity measures is relevant for future studies examining the coupling between structural and functional connectivity in healthy aging and disease.

The observations in our sample of clinically normal older adults may reflect early changes in brain connectivity that occur before functional consequences become clinically manifest. We found that greater decoupling of structural and functional connectivity was related to poorer cognitive performance, in particular to episodic memory and executive functioning. Decoupling of PCC-MPFC connectivity during rest may reflect reorganization of functional networks, which in turn may impact the ability to coordinate DN activity during cognitive tasks. Involvement of the DN in memory and executive functioning has been demonstrated by numerous studies assessing both functional connectivity (Daselaar et al., 2004; Raichle et al., 2001; Vannini et al., 2011) and structural connectivity (Metzler-Baddeley et al., 2012; O'Sullivan et al., 2005; van der Holst et al., 2013). Due to the cross-sectional design of our study we are not able to determine whether the decoupling of structural and functional networks will predict future cognitive decline or whether the breakdown in structural and functional networks progresses at a similar rate. Longitudinal studies will be necessary to determine the temporal relationship between structural and functional connectivity.

One limitation of our study is that we sampled only individuals who remain within the normal range of cognition. The observed phenomenon of decoupling of structural and functional connectivity in individuals with high WMH load may, in part, result from this sampling. Whether decoupling is also observed when global white matter injury becomes symptomatic remains to be investigated. Severe white matter injury throughout the whole network may be observed as stronger coupling of structure and function due to substantial impairment in both. Alternatively, decoupling might be observed due to floor effects on either the structural or functional connectivity measure, if accompanied by some preservation of the other measure. Examination of Table 2 and Figure 3 indicates that our sample of individuals with high WMH load were not at floor for either functional connectivity or MD measures. Another limitation of this study is that we had no measures of cerebral blood flow or vasoreactivity and so were unable to assess how the degree of neurovascular coupling may impact our functional connectivity measurements across the WMH load groups. It is also not clear to what extent regional white matter abnormalities may have affected the fiber tractography measurements. Because the tract volume estimates were not different between WMH groups, it is likely that the impact of diffusion alterations on the fiber tractography results across the groups was limited.

In summary, these results demonstrate a decoupling of structural and functional DN connectivity that accompanies higher WMH load in clinically normal older individuals and is associated with poorer cognitive performance. This decoupling may reflect reorganization of functional networks in response to global white matter pathology and may therefore provide an early marker of clinically relevant alterations in brain connectivity.

Supplementary Material

Refer to Web version on PubMed Central for supplementary material.

Acknowledgements

We thank all the collaborators and contributors to the Harvard Aging Brain Study (http://www.martinos.org/harvardagingbrain/Acknowledgements.html) and Meike Vernooij for her insightful comments on this manuscript.

Funding

Funding was provided by National Institute on Aging grants P01 AG036694, P50 AG005134, and K01 AG040197. This research was carried out in part at the Athinoula A. Martinos Center for Biomedical Imaging at the Massachusetts General Hospital, using resources provided by the Center for Functional Neuroimaging Technologies, P41 EB015896, a P41 Biotechnology Resource Grant supported by the National Institute of Biomedical Imaging and Bioengineering (NIBIB), National Institutes of Health. This work also involved the use of instrumentation supported by the NIH Shared Instrumentation Grant Program and/or High-End Instrumentation Grant Program; specifically, grant numbers S10 RR023401 and S10 RR023043. The research of A.L. is supported by VIDI Grant 639.072.411 from the Netherlands Organisation for Scientific Research (NWO).

References

Andrews-Hanna JR, Snyder AZ, Vincent JL, Lustig C, Head D, Raichle ME, Buckner RL. Disruption of large-scale brain systems in advanced aging. Neuron. 2007; 56:924–935. [PubMed: 18054866]

Catani M, Thiebaut de Schotten M. A diffusion tensor imaging tractography atlas for virtual in vivo dissections. Cortex. 2008; 44:1105–1132. [PubMed: 18619589]

Charlton RA, Barrick TR, McIntyre DJ, Shen Y, O'Sullivan M, Howe FA, Clark CA, Morris RG, Markus HS. White matter damage on diffusion tensor imaging correlates with age-related cognitive decline. Neurology. 2006; 66:217–222. [PubMed: 16434657]

Chhatwal JP, Sperling RA. Functional MRI of mnemonic networks across the spectrum of normal aging, mild cognitive impairment, and alzheimer's disease. Journal of Alzheimer's Disease. 2012; 31(Suppl 3):S155–67.

Damoiseaux JS, Greicius MD. Greater than the sum of its parts: A review of studies combining structural connectivity and resting-state functional connectivity. Brain Structure & Function. 2009; 213:525–533. [PubMed: 19565262]

Damoiseaux JS, Beckmann CF, Arigita EJ, Barkhof F, Scheltens P, Stam CJ, Smith SM, Rombouts SA. Reduced resting-state brain activity in the “default network” in normal aging. Cerebral Cortex. 2008; 18:1856–1864. [PubMed: 18063564]

Daselaar SM, Prince SE, Cabeza R. When less means more: Deactivations during encoding that predict subsequent memory. NeuroImage. 2004; 23:921–927. [PubMed: 15528092]

Fazekas F, Chawluk JB, Alavi A, Hurtig HI, Zimmerman RA. MR signal abnormalities at 1.5 T in alzheimer's dementia and normal aging. American Journal of Roentgenology. 1987; 149:351–356. [PubMed: 3496763]

Ferreira LK, Busatto GF. Resting-state functional connectivity in normal brain aging. Neuroscience and Biobehavioral Reviews. 2013; 37:384–400. [PubMed: 23333262]

Fischl B, Dale AM. Measuring the thickness of the human cerebral cortex from magnetic resonance images. Proc. Nat. Acad. Sci. U.S.A. 2000; 97:11050–11055.

Folstein MF, Folstein SE, McHugh PR. Mini-mental state. A practical method for grading the cognitive state of patients for the clinician. J. Psychiatr. Res. 1975; 12:189–98. [PubMed: 1202204]

Fox MD, Corbetta M, Snyder AZ, Vincent JL, Raichle ME. Spontaneous neuronal activity distinguishes human dorsal and ventral attention systems. Proc. Nat. Acad. Sci. U.S.A. 2006; 103:10046–10051.

Freire L, Mangin JF. Motion correction algorithms may create spurious brain activations in the absence of subject motion. NeuroImage. 2001; 14:709–722. [PubMed: 11506543]

Gouw AA, van der Flier WM, van Straaten EC, Barkhof F, Ferro JM, Baezner H, Pantoni L, Inzitari D, Erkinjuntti T, Wahlund LO. Simple versus complex assessment of white matter hyperintensities in relation to physical performance and cognition: The LADIS study. J. Neurol. 2006; 253:1189–1196. others. [PubMed: 16998647]

Greicius MD, Supekar K, Menon V, Dougherty RF. Resting-state functional connectivity reflects structural connectivity in the default mode network. Cerebral Cortex. 2009; 19:72–78. [PubMed: 18403396]

Greicius MD, Srivastava G, Reiss AL, Menon V. Default-mode network activity distinguishes alzheimer's disease from healthy aging: Evidence from functional MRI. Proc. Nat. Acad. Sci. U.S.A. 2004; 101:4637–4642.

Hedden T, Van Dijk KR, Shire EH, Sperling RA, Johnson KA, Buckner RL. Failure to modulate attentional control in advanced aging linked to white matter pathology. Cerebral Cortex. 2012; 22:1038–1051. [PubMed: 21765181]

Hedden T, Schultz AP, Rieckmann A, Mormino EC, Johnson KA, Sperling RA, Buckner RL. Multiple brain markers are linked to age-related variation in cognition. Cerebral Cortex. 2014 In press.

Homayoon N, Ropele S, Hofer E, Schwingenschuh P, Seiler S, Schmidt R. Microstructural tissue damage in normal appearing brain tissue accumulates with framingham stroke risk profile score: Magnetization transfer imaging results of the austrian stroke prevention study. Clin. Neurol. Neurosurg. 2013; 115:1317–1321. [PubMed: 23298976]

Honey CJ, Sporns O, Cammoun L, Gigandet X, Thiran JP, Meuli R, Hagmann P. Predicting human resting-state functional connectivity from structural connectivity. Proc. Nat. Acad. Sci. U.S.A. 2009; 106:2035–2040.

Jeurissen B, Leemans A, Jones DK, Tournier JD, Sijbers J. Probabilistic fiber tracking using the residual bootstrap with constrained spherical deconvolution. Human Brain Mapping. 2011; 32:461–479. [PubMed: 21319270]

Johansen-Berg H. Imaging the relationship between structure, function and behaviour in the human brain. Brain Structure & Function. 2009; 213:499–500. [PubMed: 19779738]

Jones DK, Leemans A. Diffusion tensor imaging. Methods in Molecular Biology. Clifton, N.J. 2011; 711:127–144.

Jones DK, Christiansen KF, Chapman RJ, Aggleton JP. Distinct subdivisions of the cingulum bundle revealed by diffusion MRI fibre tracking: Implications for neuropsychological investigations. Neuropsychologia. 2013; 51:67–78. [PubMed: 23178227]

Kristo G, Leemans A, Raemaekers M, Rutten GJ, de Gelder B, Ramsey NF. Reliability of two clinically relevant fiber pathways reconstructed with constrained spherical deconvolution. Mag. Res. Med. 2013; 70:1544–1556.

Lebel C, Walker L, Leemans A, Phillips L, Beaulieu C. Microstructural maturation of the human brain from childhood to adulthood. NeuroImage. 2008; 40:1044–1055. [PubMed: 18295509]

Leemans A, Jones DK. The B-matrix must be rotated when correcting for subject motion in DTI data. Mag. Res. Med. 2009; 61:1336–1349.

Leemans A, Jeurissen B, Sijbers J, Jones DK. ExploreDTI: A graphicaltoolbox forprocessing, analyzing, and visualizing diffusion MR data. 17th Annual Meeting of Intl. Soc. Mag. Reson. Med. 2009:3537.

Leritz EC, Shepel J, Williams VJ, Lipsitz LA, McGlinchey RE, Milberg WP, Salat DH. Associations between T1 white matter lesion volume and regional white matter microstructure in aging. Human Brain Mapping. 2014; 35:1085–1100. [PubMed: 23362153]

Lustig C, Snyder AZ, Bhakta M, O'Brien KC, McAvoy M, Raichle ME, Morris JC, Buckner RL. Functional deactivations: Change with age and dementia of the alzheimer type. Proc. Nat. Acad. Sci. U.S.A. 2003; 100:14504–14509.

Metzler-Baddeley C, Jones DK, Steventon J, Westacott L, Aggleton JP, O'Sullivan MJ. Cingulum microstructure predicts cognitive control in older age and mild cognitive impairment. J. Neurosci. 2012; 32:17612–17619. [PubMed: 23223284]

O'Sullivan M, Barrick TR, Morris RG, Clark CA, Markus HS. Damage within a network of white matter regions underlies executive dysfunction in CADASIL. Neurology. 2005; 65:1584–1590. [PubMed: 16301485]

O'Sullivan M, Summers PE, Jones DK, Jarosz JM, Williams SC, Markus HS. Normal-appearing white matter in ischemic leukoaraiosis: A diffusion tensor MRI study. Neurology. 2001; 57:2307–2310. [PubMed: 11756617]

Pfefferbaum A, Adalsteinsson E, Sullivan EV. Frontal circuitry degradation marks healthy adult aging: Evidence from diffusion tensor imaging. NeuroImage. 2005; 26:891–899. [PubMed: 15955499]

Power JD, Barnes KA, Snyder AZ, Schlaggar BL, Petersen SE. Spurious but systematic correlations in functional connectivity MRI networks arise from subject motion. NeuroImage. 2012; 59:2142–2154. [PubMed: 22019881]

Raichle ME, MacLeod AM, Snyder AZ, Powers WJ, Gusnard DA, Shulman GL. A default mode of brain function. Proc. Nat. Acad. Sci. U.S.A. 2001; 98:676–682.

Reijmer YD, Leemans A, Heringa SM, Wielaard I, Jeurissen B, Koek HL, Biessels GJ, Vascular Cognitive Impairment Study group. Improved sensitivity to cerebral white matter abnormalities in alzheimer's disease with spherical deconvolution based tractography. PloS One. 2012; 7:e44074. [PubMed: 22952880]

Rohde GK, Barnett AS, Basser PJ, Marenco S, Pierpaoli C. Comprehensive approach for correction of motion and distortion in diffusion-weighted MRI. Mag. Res. Med. 2004; 51:103–114.

Salat DH, Tuch DS, Hevelone ND, Fischl B, Corkin S, Rosas HD, Dale AM. Age-related changes in prefrontal white matter measured by diffusion tensor imaging. Ann. N. Y. Acad. Sci. 2005; 1064:37–49. [PubMed: 16394146]

Schultz AP, Chhatwal JP, Huijbers W, Hedden T, van Dijk KR, McLaren DG, Ward AM, Wigman S, Sperling RA. Template based rotation: A method for functional connectivity analysis with a priori templates. NeuroImage. 2014; 102P2:620–636. [PubMed: 25150630]

Skudlarski P, Jagannathan K, Anderson K, Stevens MC, Calhoun VD, Skudlarska BA, Pearlson G. Brain connectivity is not only lower but different in schizophrenia: A combined anatomical and functional approach. Biological Psychiatry. 2010; 68:61–69. [PubMed: 20497901]

Tax CM, Jeurissen B, Vos SB, Viergever MA, Leemans A. Recursive calibration of the fiber response function for spherical deconvolution of diffusion MRI data. NeuroImage. 2014; 86:67–80. [PubMed: 23927905]

Tournier JD, Calamante F, Connelly A. Robust determination of the fibre orientation distribution in diffusion MRI: Non-negativity constrained super-resolved spherical deconvolution. NeuroImage. 2007; 35:1459–1472. [PubMed: 17379540]

van den Heuvel M, Mandl R, Luigjes J, Hulshoff Pol H. Microstructural organization of the cingulum tract and the level of default mode functional connectivity. J. Neurosci. 2008; 28:10844–10851. [PubMed: 18945892]

van der Holst HM, Tuladhar AM, van Norden AG, de Laat KF, van Uden IW, van Oudheusden LJ, Zwiers MP, Norris DG, Kessels RP, de Leeuw FE. Microstructural integrity of the cingulum is related to verbal memory performance in elderly with cerebral small vessel disease: The RUN DMC study. NeuroImage. 2013; 65:416–423. [PubMed: 23032491]

Van Dijk KR, Sabuncu MR, Buckner RL. The influence of head motion on intrinsic functional connectivity MRI. NeuroImage. 2012; 59:431–438. [PubMed: 21810475]

Van Dijk KR, Hedden T, Venkataraman A, Evans KC, Lazar SW, Buckner RL. Intrinsic functional connectivity as a tool for human connectomics: Theory, properties, and optimization. Journal of Neurophysiology. 2010; 103:297–321. [PubMed: 19889849]

Vannini P, O'Brien J, O'Keefe K, Pihlajamaki M, Laviolette P, Sperling RA. What goes down must come up: Role of the posteromedial cortices in encoding and retrieval. Cerebral Cortex. 2011; 21:22–34. [PubMed: 20363808]

Vernooij MW, Ikram MA, Vrooman HA, Wielopolski PA, Krestin GP, Hofman A, Niessen WJ, van der Lugt A, Breteler MM. White matter microstructural integrity and cognitive function in a general elderly population. Arch. Gen. Psychiatry. 2009; 66:545–553. [PubMed: 19414714]

Wakana S, Jiang H, Nagae-Poetscher LM, van Zijl PC, Mori S. Fiber tract-based atlas of human white matter anatomy. Radiology. 2004; 230:77–87. [PubMed: 14645885]

Wang Z, Dai Z, Gong G, Zhou C, He Y. Understanding structural-functional relationships in the human brain: A large-scale network perspective. Neuroscientist. 2014 In press.

Ward AM, Mormino EC, Huijbers W, Schultz AP, Hedden T, Sperling RA. Relationships between default-mode network connectivity, medial temporal lobe structure, and age-related memory deficits. Neurobiol Aging. 2015; 36:265–72. [PubMed: 25113793]

Zhang Z, Liao W, Chen H, Mantini D, Ding JR, Xu Q, Wang Z, Yuan C, Chen G, Jiao Q. Altered functional-structural coupling of large-scale brain networks in idiopathic generalized epilepsy. Brain. 2011; 134:2912–2928. others. [PubMed: 21975588]

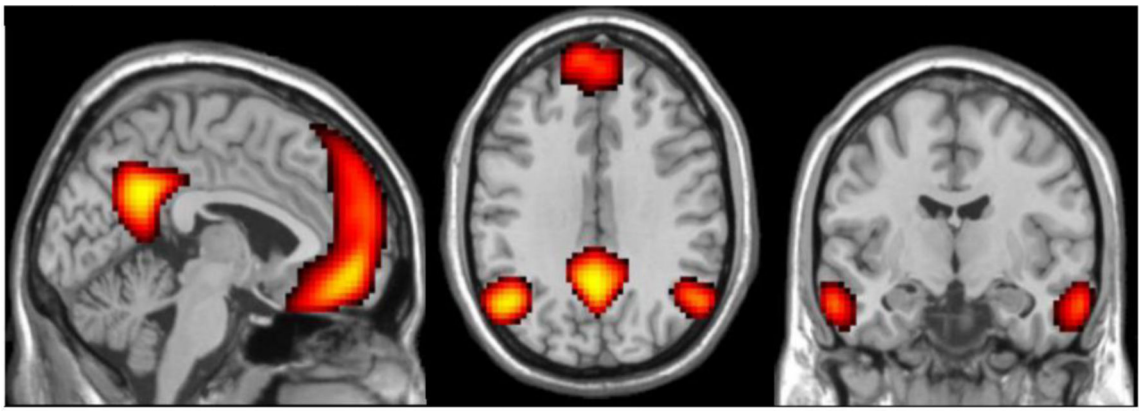

Figure 1. Template of the default mode network

The template of the default network (DN) was created from an independent set of 675 young subjects (Schultz et al. 2014). All regions represent areas of DN connectivity of $p < 0.001$ (FDR corrected), including the posterior cingulate cortex (PCC) and medial prefrontal cortex (MPFC) (left panel). For each subject, the functional connectivity between the PCC and MPFC of the DN was calculated as the correlation between the average BOLD time-course of each region.

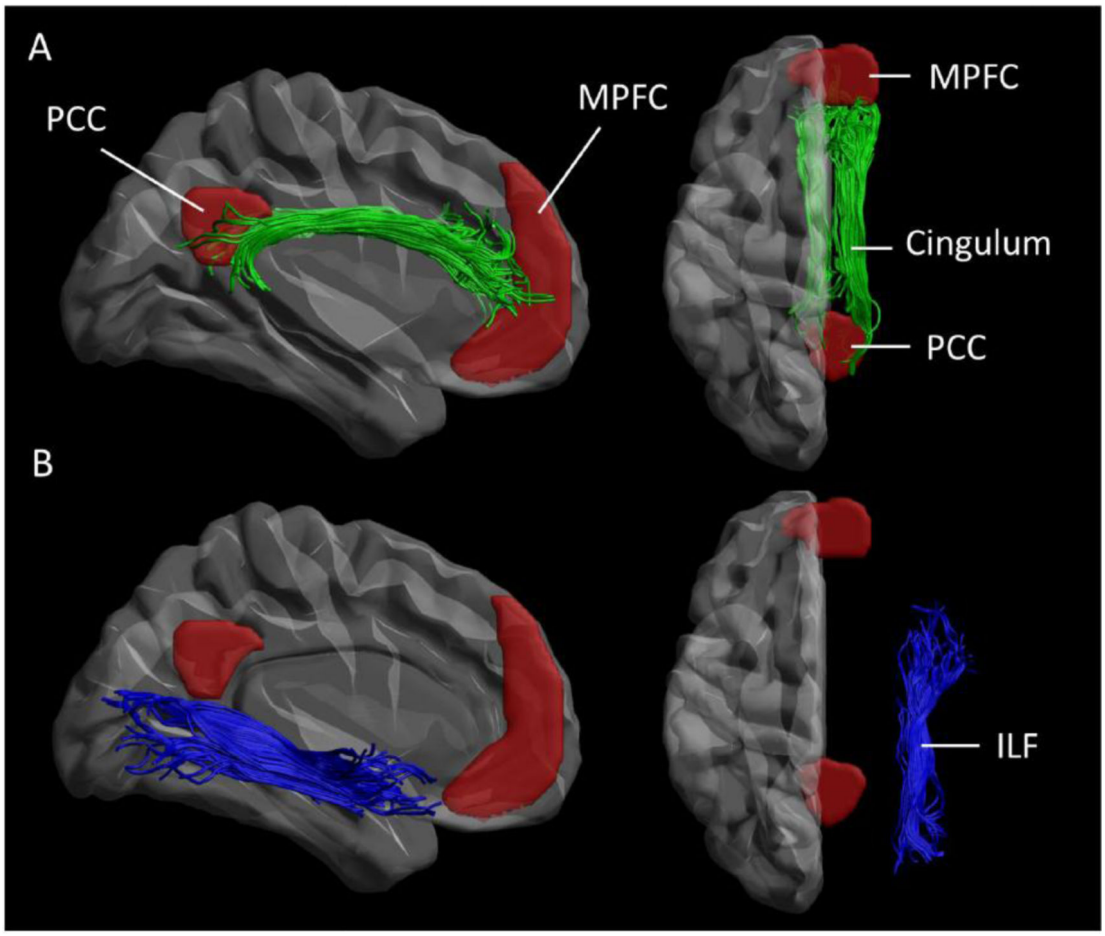

Figure 2. The cingulum bundle and inferior longitudinal fasciculus

The cingulum bundle and right inferior longitudinal fasciculus (ILF) were parcellated from the whole brain fiber tractography maps using standardized regions of interest for tract selection. A) Sagittal and axial view of the cingulum bundle (green). The cingulum connects the posterior cingulate cortex (PCC) and medial prefrontal cortex (MPFC) node of the default network indicated in red (Greicius et al. 2010, van den Heuvel et al. 2009). B) The ILF (blue), not passing through the PCC or MPFC, served as a control tract. Results are projected on a normalized brain.

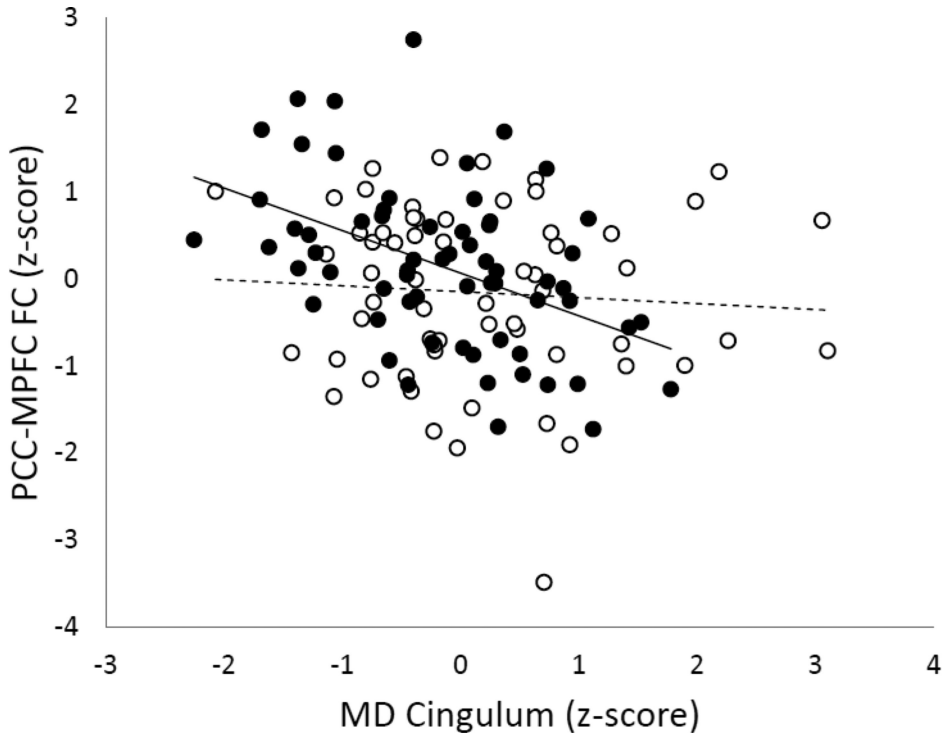

Figure 3. The relationship between PCC-MPFC functional connectivity and cingulum MD

The correlation is shown for individuals with low WMH load (filled circles, solid line) and with high WMH load (open circles, dashed line). Units are z-scores corrected for age, sex, average movement, SNR, and the number of outlier volumes scrubbed from each fMRI data set.

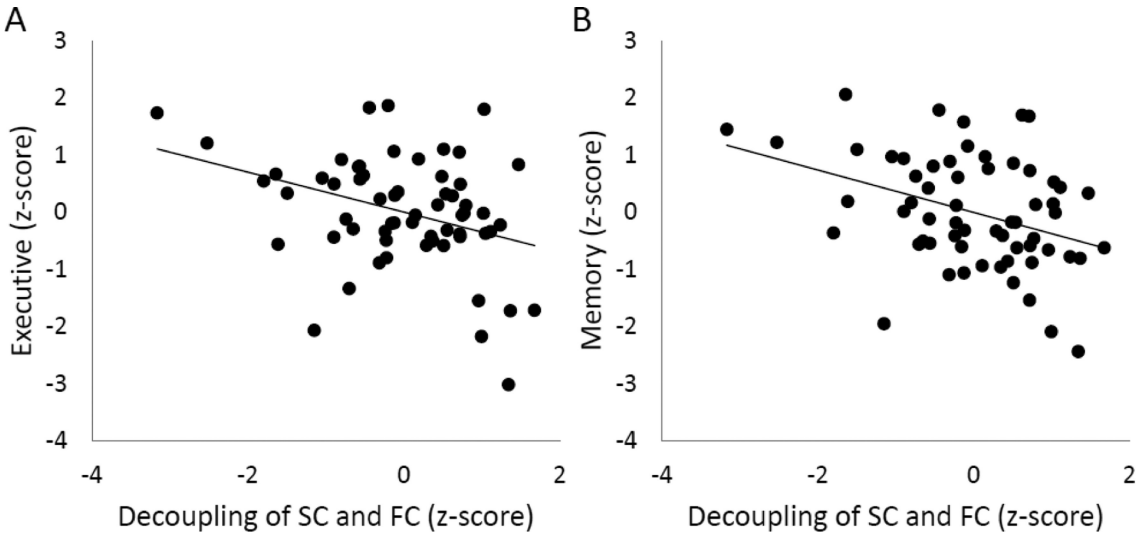

Figure 4. The relationship between decoupling of PCC-MPFC structural and functional connectivity and cognition in individuals with high WMH load

Correlation plots show that greater decoupling of PCC-MPFC structural and functional connectivity is related to worse performance on executive functioning (A) and memory (B). Units are z-scores corrected for age and sex.

Table 1

Characteristics of the study sample

	Low WMH load N=64	High WMH load N=61
Age, year	71.9 ± 5.5	75.4 ± 5.6**
Gender, % male	38	36
Fazekas WMH score 0/1, %	0/100	-
Fazekas WMH score 2/3, %	-	77/23
Total brain volume, cc	1003 ± 103	994 ± 91
Hypertension[a], %	73	85
Structural and functional connectivity		
PCC vs. MPFC[b]	0.49 ± 0.23	0.34 ± 0.34**
Cingulum FA	0.35 ± 0.03	0.34 ± 0.04*
Cingulum MD	0.88 ± 0.05	0.92 ± 0.07**
ILF FA	0.36 ± 0.03	0.35 ± 0.03
ILF MD	0.92 ± 0.06	0.98 ± 0.09**
Whole WM FA excl. cingulum	0.40 ± 0.01	0.39 ± 0.01
Whole WM MD excl. cingulum	0.89 ± 0.02	0.92 ± 0.04**
Cingulum volume[c]	229 ± 74	243 ± 123
ILF volume[c]	327 ± 182	298 ± 148
Cognition (z-scores)		
Processing speed	0.27 ± 1.01	−0.42 ± 1.07**
Executive functioning	0.27 ± 1.02	−0.41 ± 1.01**
Memory	0.32 ± 0.93	−0.22 ± 0.96**

Data are mean ± SD or percentages. White matter hyperintensity (WMH) load was quantified according to the Fazekas score (Fazekas et al. 1987). PCC= posterior cingulated cortex; MPFC= medial prefrontal cortex; ILF= inferior longitudinal fasciculus; FA = fractional anisotropy; MD = mean diffusivity (10^{-3} mm^2/s).

[a]Hypertension was defined as systolic blood pressure ≥140, diastolic blood pressure ≥90 or the use of antihypertensive medication.

[b]The mean correlation coefficient of PCC-MPFC connectivity before Fisher's r-to-z transformation.

[c]Tract volume is indicated by the number of streamlines.

*p<0.05

**P<0.01.

Table 2

Age- and sex adjusted between-group difference in white matter structural connectivity

	Low WMH load	High WMH load	Mean difference
Cingulum FA	0.19 ± 0.13	−0.21 ± 0.13	−0.40 ± 0.19*
Cingulum MD	−0.19 ± 0.11	0.20 ± 0.12	0.39 ± 0.17*
Whole WM FA excl. cingulum	0.20 ± 0.12	−0.21 ± 0.12	−0.41 ± 0.17*
Whole WM MD excl. cingulum	−0.47 ± 0.11	0.49 ± 0.11	0.96 ± 0.15**

Age- and sex adjusted standardized (z-score) ± SE are shown of FA and MD of the cingulum bundle and of the whole white matter (WM) excluding the cingulum bundle.

* $p<0.05$

** $P<0.01$.